Supporting Information

Visualization of sub-nanometer scale multi-orientational ordering in thin films of polymer/non-fullerene acceptor blends

Urvashi Bothra[abc], Pramiti Hui[d], Wen Liang Tan[c], Eliot Gann[e], Hariprasad Venugopal[f], Chandramouli Subramaniam[d], Amelia C.Y. Liu*[g] Christopher R. McNeill*[c], and Dinesh Kabra*[b]*

[a]IITB-Monash Research Academy, IIT Bombay, Mumbai-400076, India.

[b]Department of Physics, Indian Institute of Technology Bombay, Powai, Mumbai - 400076, India.

[c]Department of Materials Science and Engineering, Monash University, Wellington Road, Clayton, Victoria, 3800, Australia.

[d]Department of Chemistry, Indian Institute of Technology Bombay, Powai, Mumbai - 400076, India.

[e]Materials Measurement Science Division, National Institute of Standards and Technology, Gaithersburg, MD 20899, USA

[f]Ramaciotti Centre for Cryo-Electron Microscopy, Monash University, Clayton, Victoria 3800, Australia

[g]School of Physics and Astronomy, Monash University, Clayton, Victoria, 3800, Australia.

KEYWORDS: non-fullerene acceptors, organic solar cells, cryo-electron microscopy, micro-Raman spectroscopy, multi-orientational packing

** Corresponding authors: Dinesh Kabra (E-mail: dkabra@iitb.ac.in)*
Christopher R. McNeill (E-mail:Christopher.mcneill@monash.edu)
Amelia C.Y. Liu (E-mail: amelia.liu@monash.edu)
Chandramouli Subramaniam (E-mail: csubbu@chem.iitb.ac.in)

This file contains Figure S1 to Figure S26 and Table S1 to Table S5.

This file also contains supplementary note 1-4.

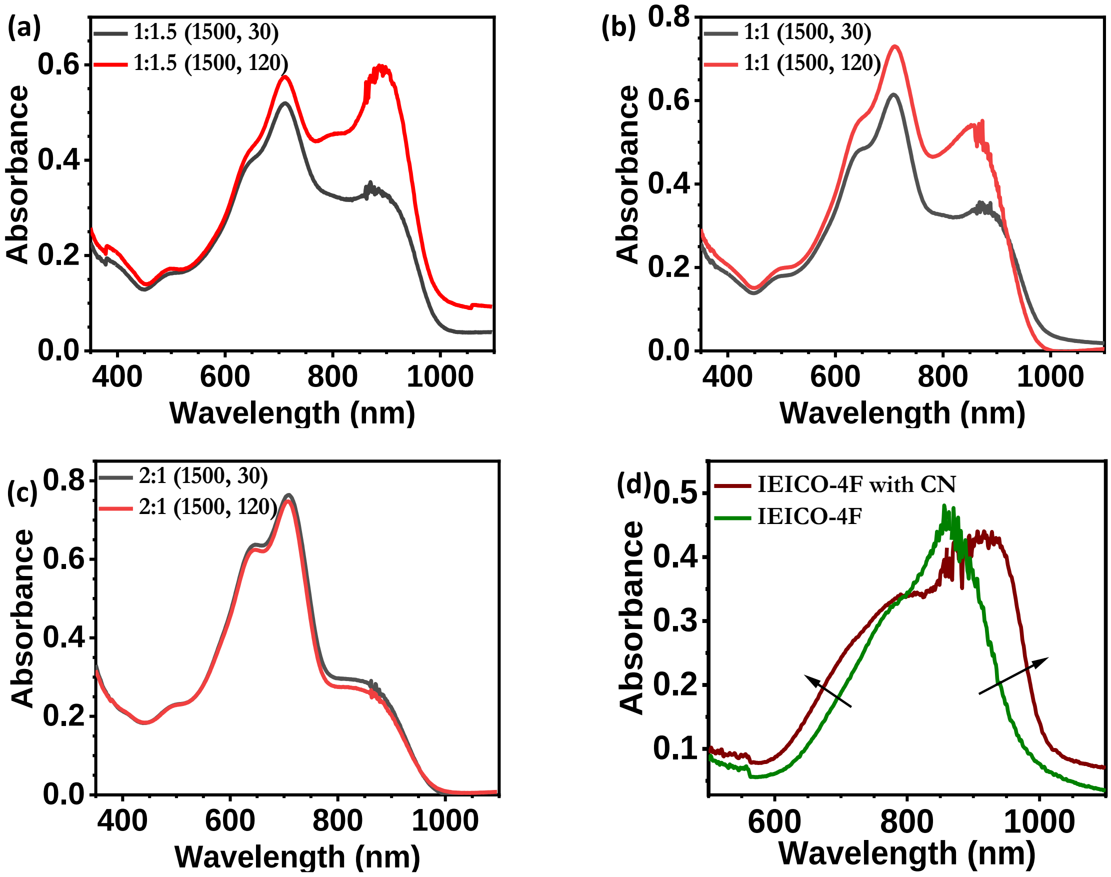

Figure S1. Absorption spectra of PTB7-Th:IEICO-4F blend film of **(a)** 1:1.5, **(b)** 1:1, and **(c)** 2:1 ratio, spin-coated at 1500 rpm for 30 and 120 seconds. **(d)** Absorption spectra of IEICO-4F film spin-coated from CB (olive) and CB with 3 vol% CN solution (wine).

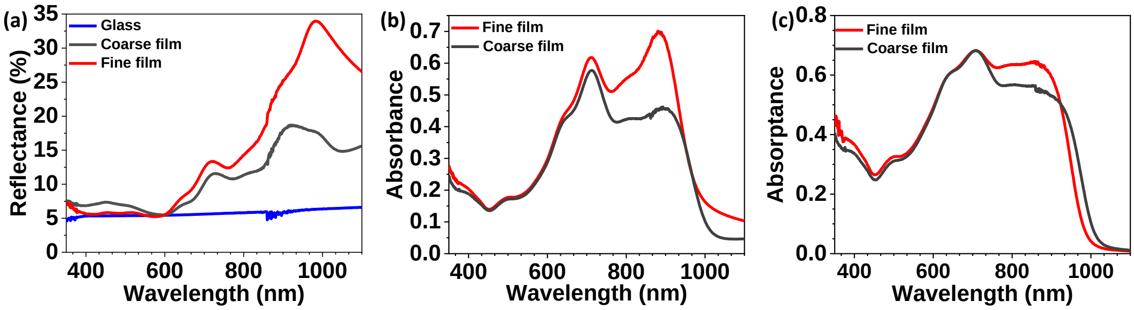

Figure S2. (a) Reflectance spectra of glass, coarse, and fine blend film. (b) Absorbance spectra and (c) absorptance spectra of coarse and fine blend film spin coated at 1500 rpm for 30 seconds and 120 seconds, respectively. Absorptance is calculated as 1-Reflection-Transmission.

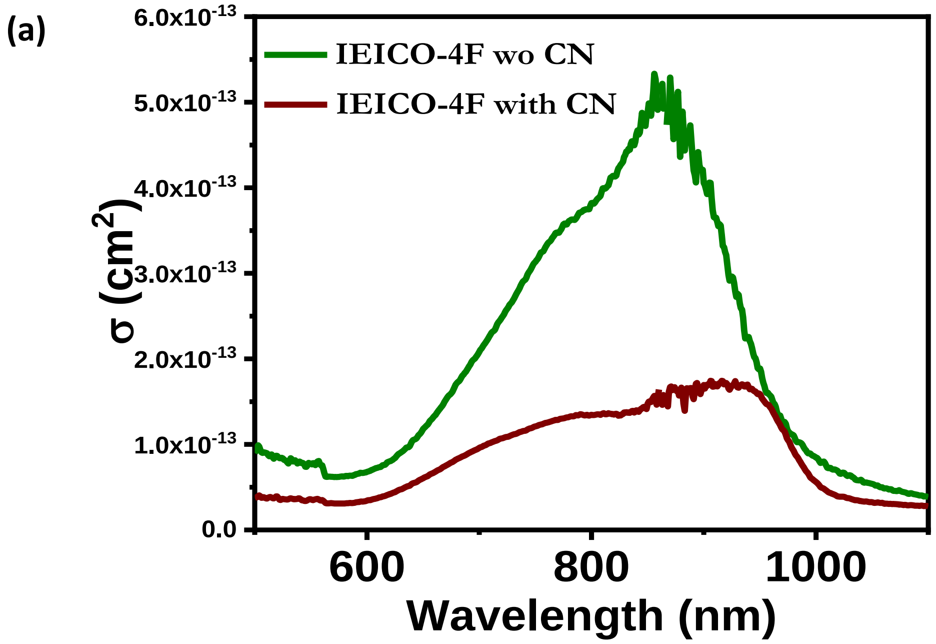

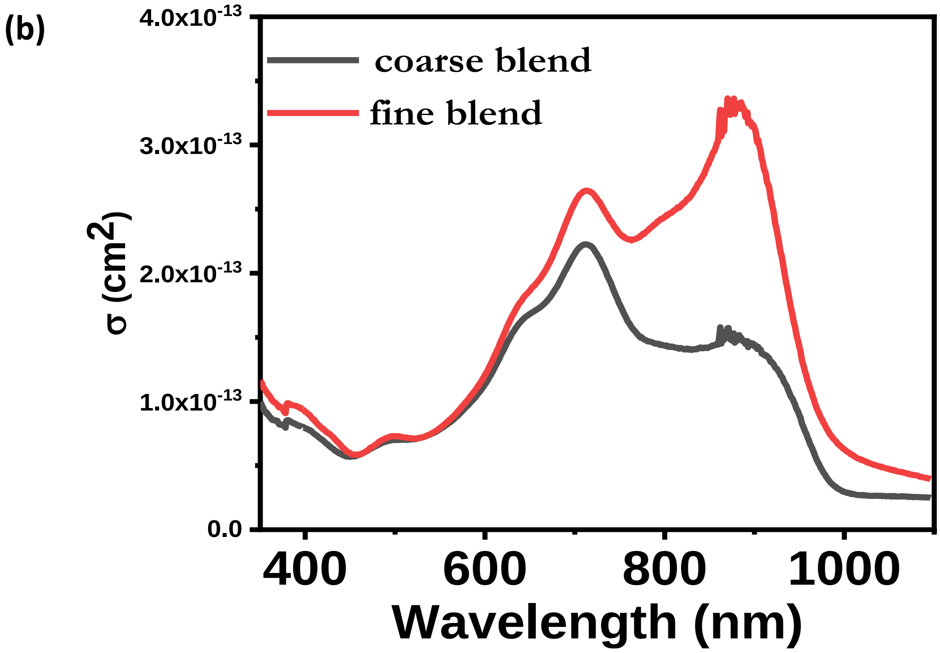

Figure S3. (a) Absorption cross-section (σ) of IEICO-4F with and without addition of 1-CN in CB, **(b)** Absorption cross-section of PTB7-Th:IEICO-4F (1:2) blend spin-coated for 30 sec (red solid line for coarse morphology) and 120 sec (black solid line for fine morphology).

Supplementary Note 1:

- The absorption cross section is given by[1]:

$\sigma\ (\mathrm{cm}^2)=1000\varepsilon(\lambda)\ln 10/N_A$

Here, $\varepsilon(\lambda)$ is the molar absorption coefficient (L mol^{-1} cm^{-1}) and N_A is the Avogadro number.

The molar absorption coefficient can be calculated from[2]:

$\varepsilon(\lambda)=0.43\alpha(\lambda)/C$

$\alpha(\lambda)$ is absorption coefficient of material

C is molar concentration of film

$\alpha(\lambda)$ is calculated from the absorbance spectra using beer lambert's law.

$2.303*A= \alpha d$

Where d is thickness of film

C is estimated from the density and molecular weight of materials.

Density of PTB7-Th is taken as 1 gm/cm^3 and of IEICO-4F is 1.2 gm/cm^3 [2,3].

Molecular weight of PTB7-Th is taken as 907.4 gm/mol and for IEICO-4F is 1808 gm/mol [2,3].

References:

1. Oyama et al. ACS Materials Lett. 2020, 2, 161−167
2. Benten et al., Energy Environ. Sci., 2016, 9, 135—140
3. Retrieved from https://www.ossila.com/products/ieico-4f

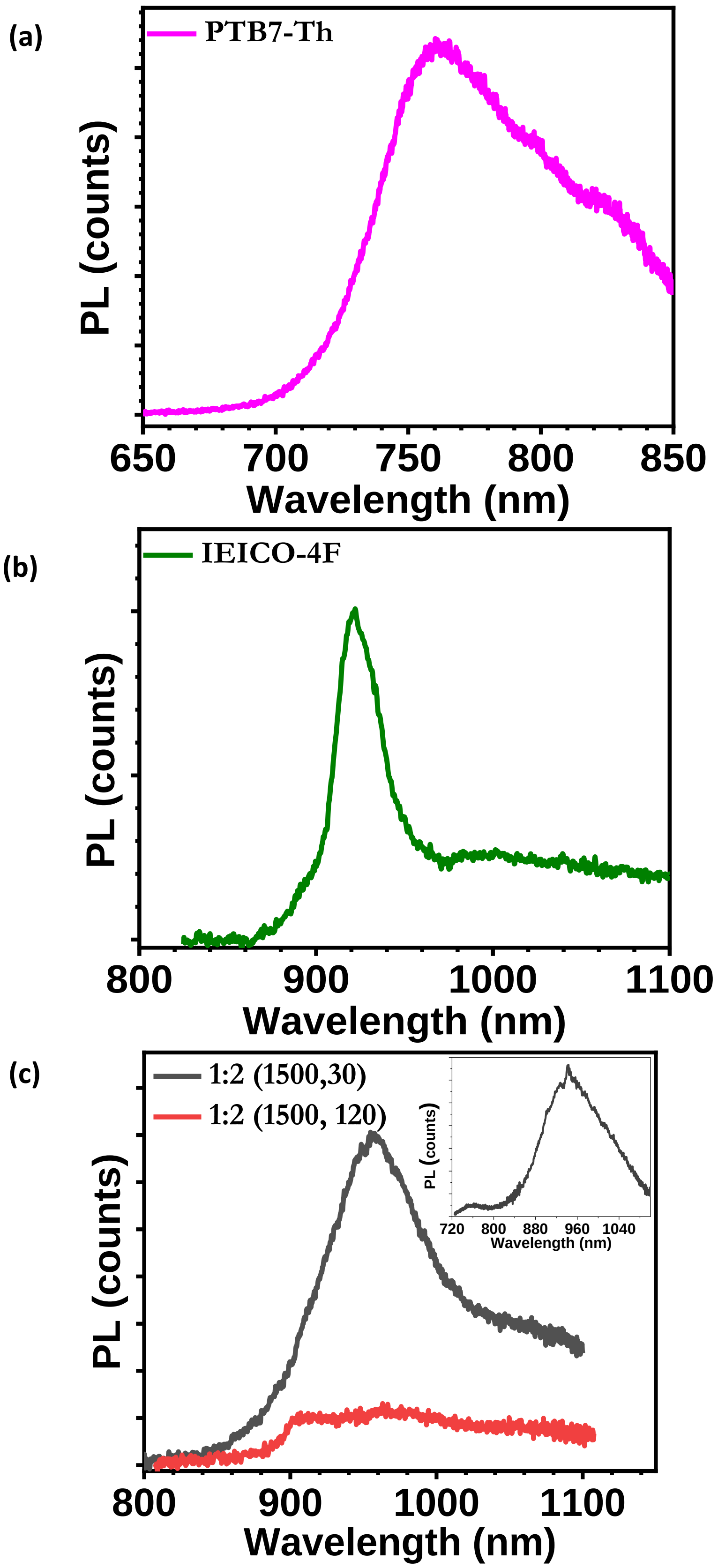

Figure S4. PL spectra of **(a)** pristine PTB7-Th and **(b)** IEICO-4F film (50 nm thick film). **(c)** PL spectra of PTB7-Th:IEICO-4F blend films (in CB+CN) spin coated at 1500 rpm for 30 seconds and 120 seconds on quartz substrates excited by 638 nm laser. **Inset:** PL spectrum from 720 nm to 1100 nm of PTB7-Th:IEICO-4F blend film spin-coated for 30 seconds.

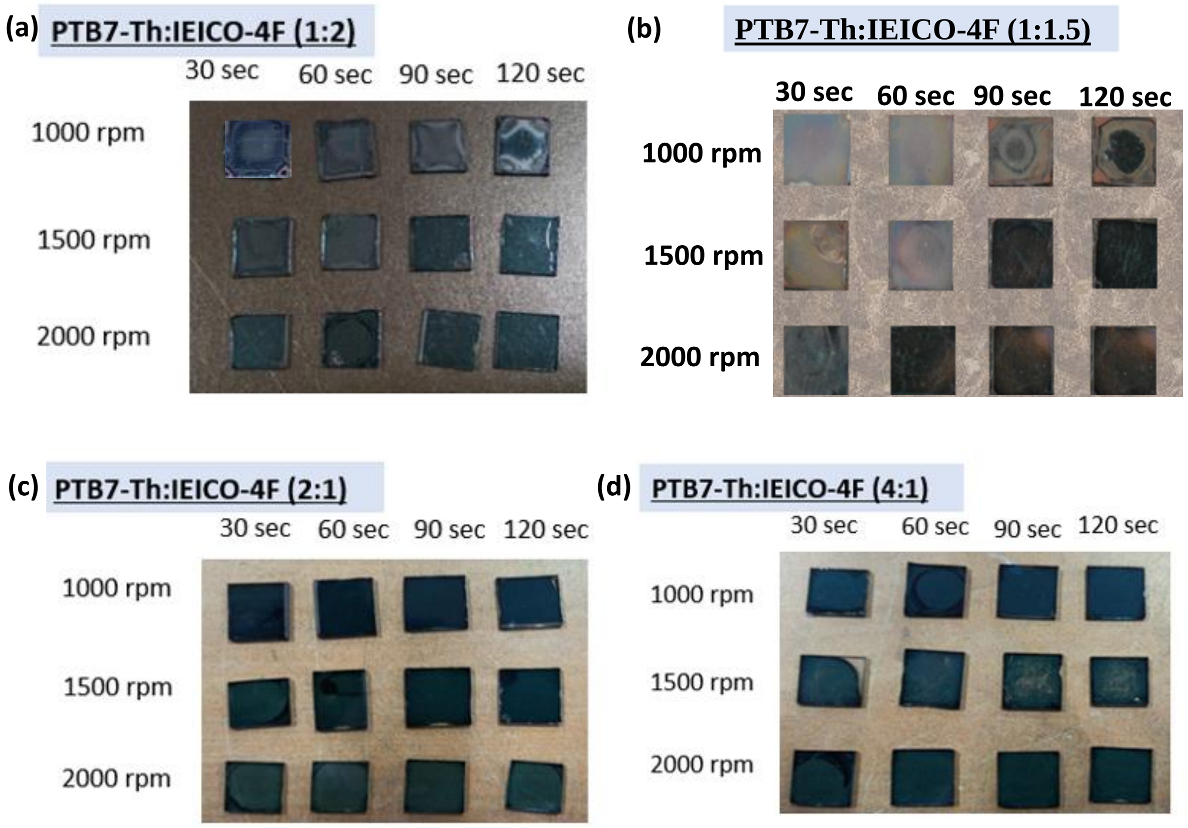

Figure S5. Digital images of PTB7-Th:IEICO-4F film at **(a)** 1:2, **(b)** 1:1.5, **(c)** 2:1 and **(d)** 4:1 blend ratio spin coated at 1000 to 2000 rpm for 30, 60, 90 and 120 seconds.

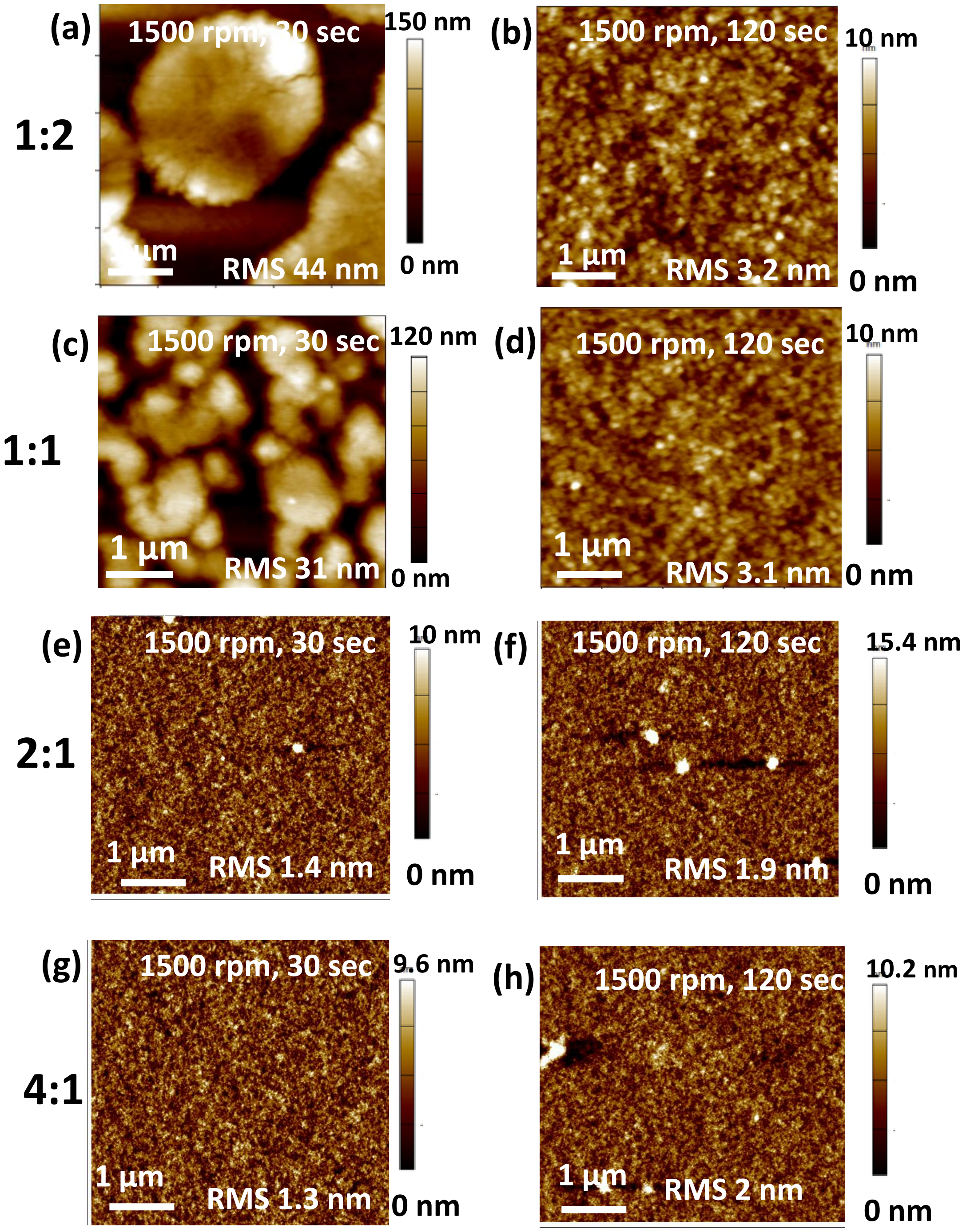

Figure S6. Morphological image (AFM) of PTB7-Th:IEICO-4F blend films spin coated at **(a,c,e,g)** 1500 rpm for 30 seconds and **(b,d,f,h)** 1500 rpm for 120 seconds. Films prepared from PTB7-Th:IEICO-4F blend with **(a,b)** 1:2, **(c,d)** 1:1, **(e,f)** 2:1 and **(g,h)** 4:1 ratio.

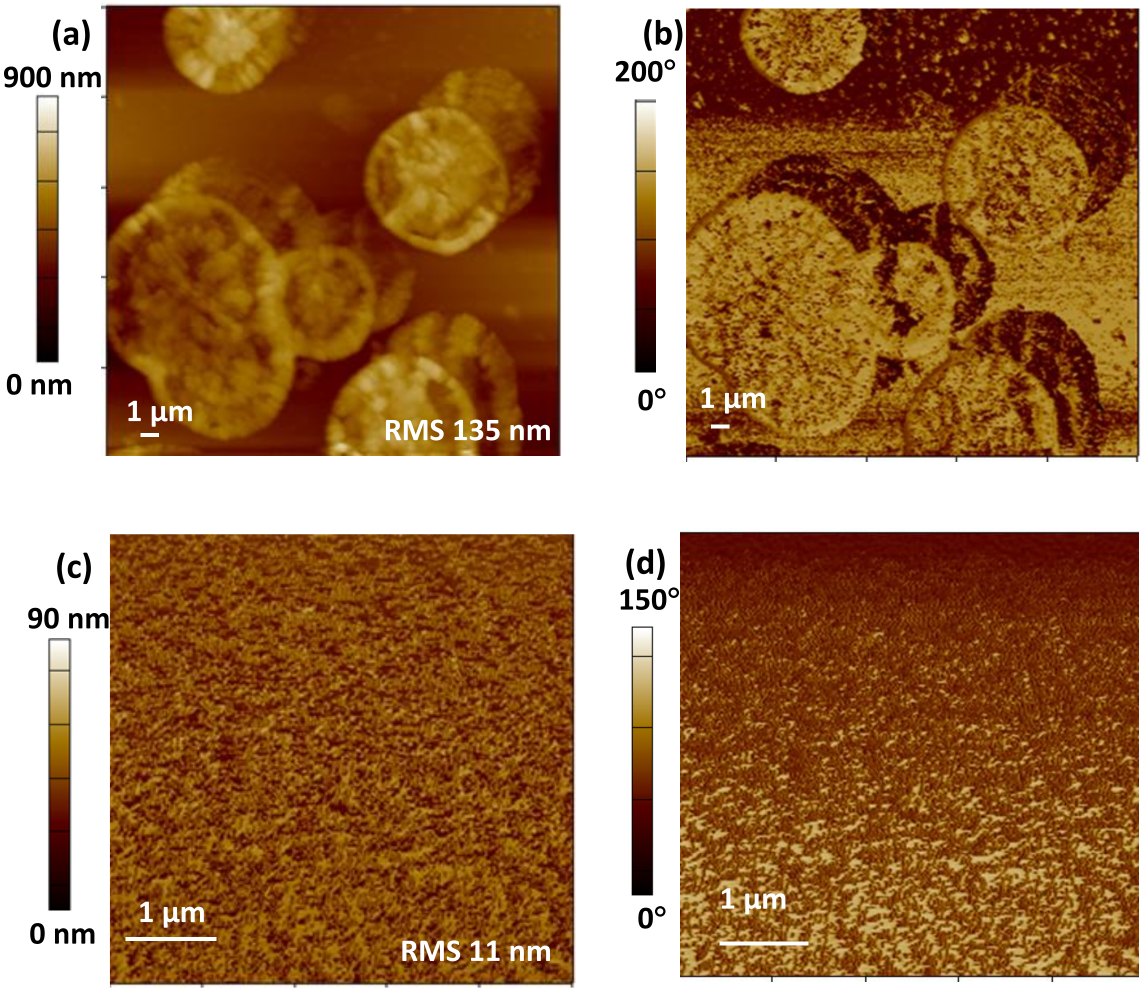

Figure S7. (a) AFM height image and **(b)** phase image of IEICO-4F film spin-coated from the solution in CB with 3 vol% of 1-CN. **(c)** AFM height image and **(d)** phase image of IEICO-4F film spin-coated from solution in CB.

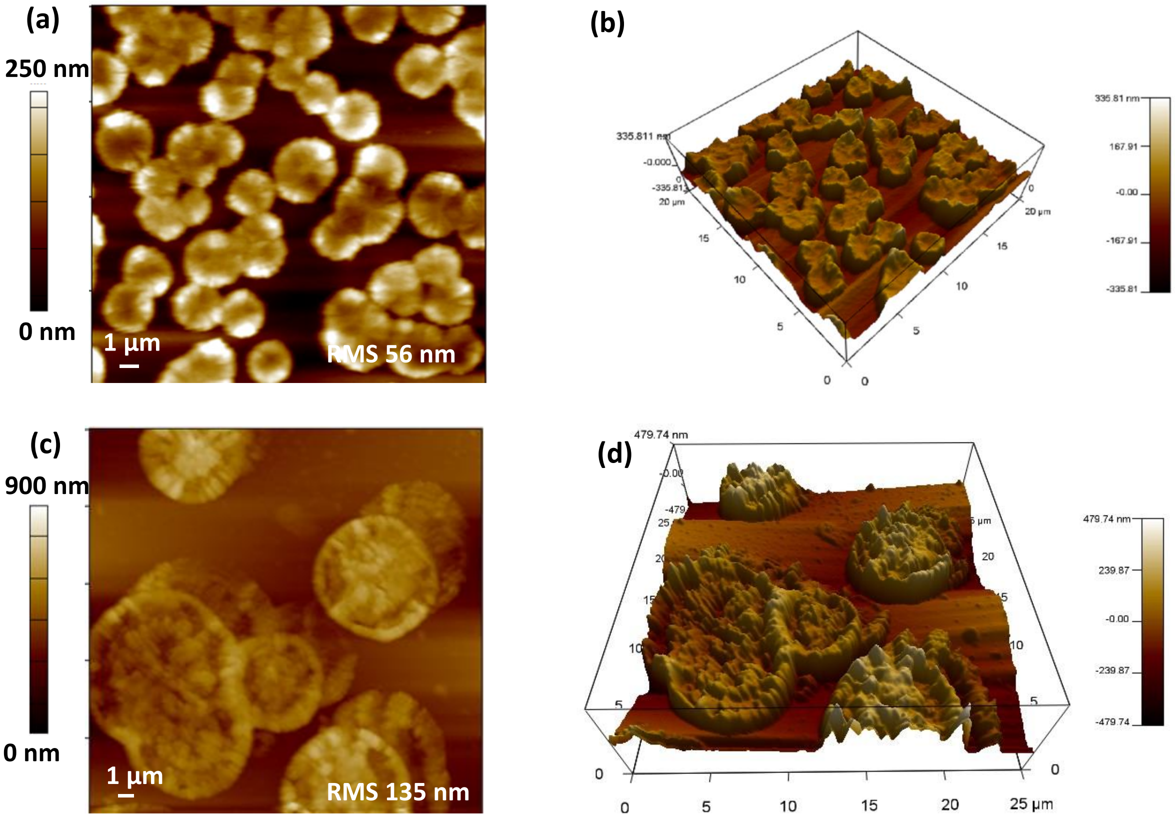

Figure S8. **(a)** AFM height image and **(b)** 3D height image of blend film spin coated for 30 seconds. **(c)** AFM height image and **(d)** 3D height image of pristine IEICO-4F film spin-coated from CB and 3 vol% 1-CN solution.

Supplementary Note 2:

The KPFM was first performed on an Au-evaporated film to determine the work function (W.F.) of the Ti/Ir tip. Figure S9(a and b) shows height and potential image of the Au film. The W.F. of a thin Au film in ambient conditions is taken as 4.7 eV[1]. The W.F. of the tip is calculated by $\phi_{tip} = -e*VCPD+\phi_{sample}$ as the voltage is applied to the tip[2]. Therefore, the W.F. of the tip is calculated as 4.46 eV; similarly, the W.F. of the blend film is obtained. We additionally measured the W.F. of pristine PTB7-Th and IEICO-4F by performing the KPFM of the drop casted solution, as shown in Figure S9(d). As expected, we found that the W.F. of IEICO-4F is higher than that of PTB7-Th and the values are similar to the W.F. reported by Karuthedath et al. [3].

References:

1. A. Kahn, *Materials Horizons* **2016**, 3, 7.
2. W. Melitz, J. Shen, A. C. Kummel, S. Lee, *Surface Science Reports* **2011**, 66, 1.
3. S. Karuthedath, J. Gorenflot, Y. Firdaus, N. Chaturvedi, C. S. P. De Castro, G. T. Harrison, J. I. Khan, A. Markina, A. H. Balawi, T. A. D. Pena, W. Liu, R. Z. Liang, A. Sharma, S. H. K. Paleti, W. Zhang, Y. Lin, E. Alarousu, D. H. Anjum, P. M. Beaujuge, S. De Wolf, I. McCulloch, T. D. Anthopoulos, D. Baran, D. Andrienko, F. Laquai, *Nat Mater* **2021**, 20, 378.

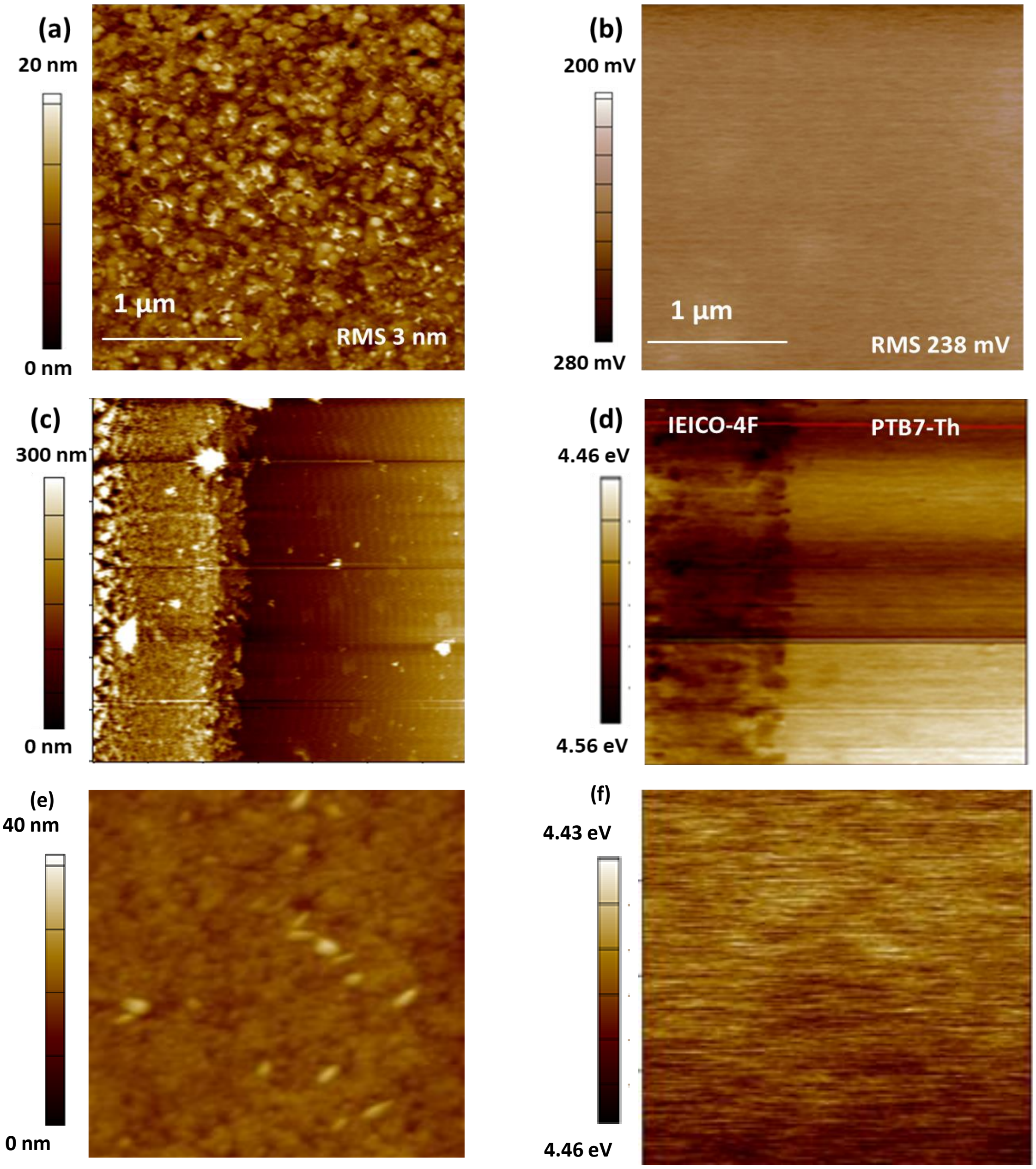

Figure S9. **(a)** AFM height image and **(b)** KPFM potential image with scale bar showing contact potential difference of Au evaporated on ITO coated glass**.** **(c)** Height image and **(d)** potential image of drop casted IEICO-4F and PTB7-Th. **(e)** AFM height image and **(f)** KPFM image for 1:1.5 blend film with fine morphology. Scale bar shows W.F. of the materials.

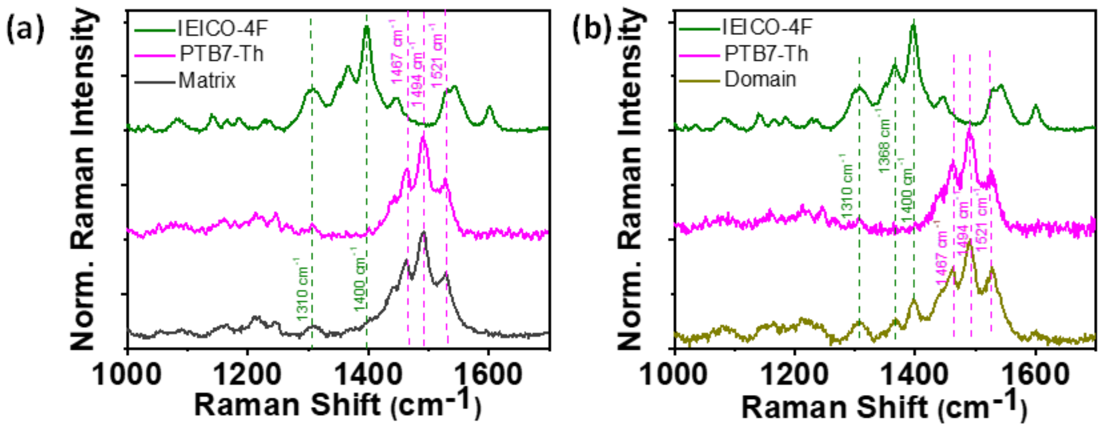

Figure S10. Normalized Raman intensity for (a) pristine PTB7-Th, pristine IEICO-4F, and matrix region of the blend film and (b) pristine PTB7-Th, pristine IEICO-4F, and coarse region of the blend film.

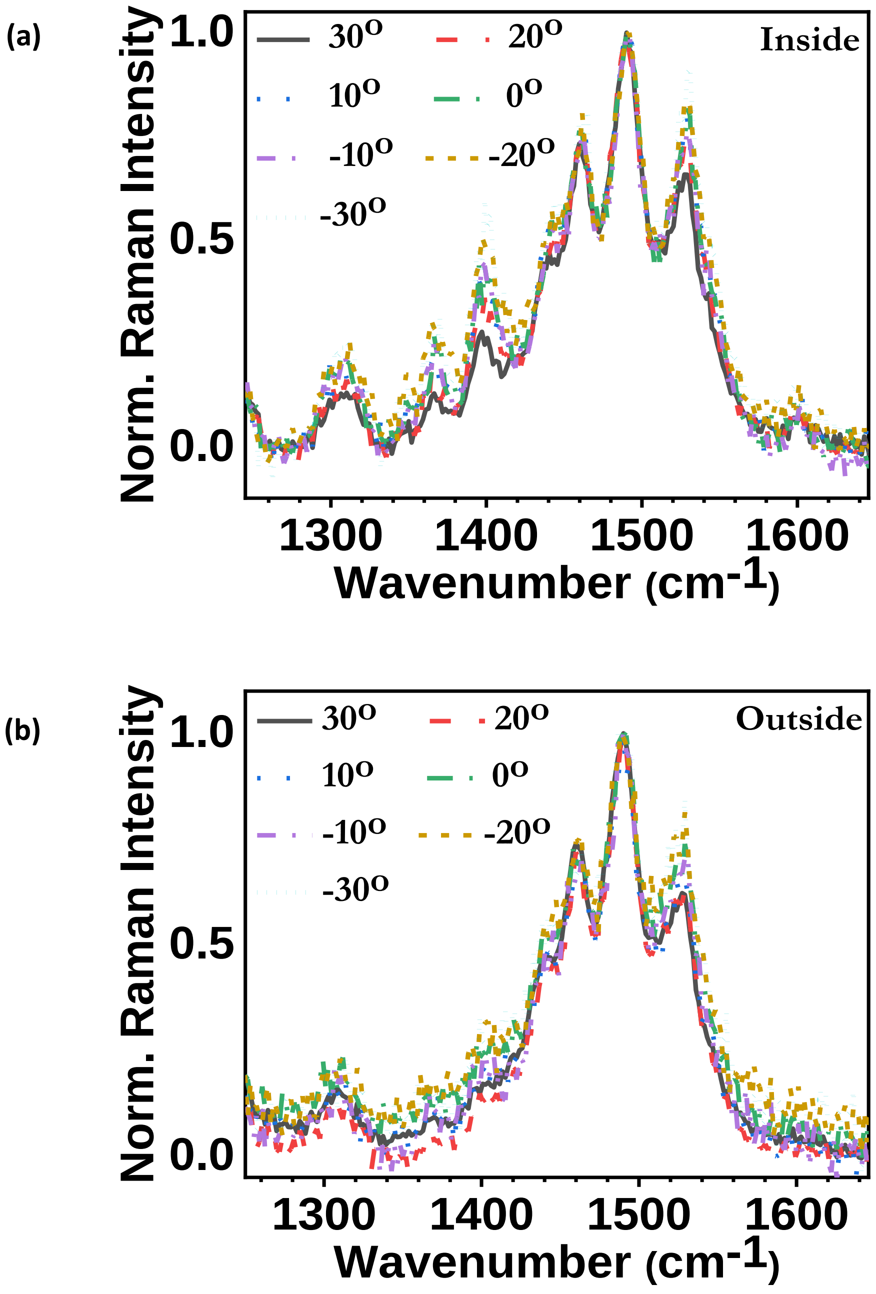

Figure S11. Polarization angle dependent Raman spectroscopy in the **(a)** inside (domain) and **(b)** outside (matrix) region of the PTB7-Th:IEICO-4F (1:1.5) domain in the blend of coarse morphology.

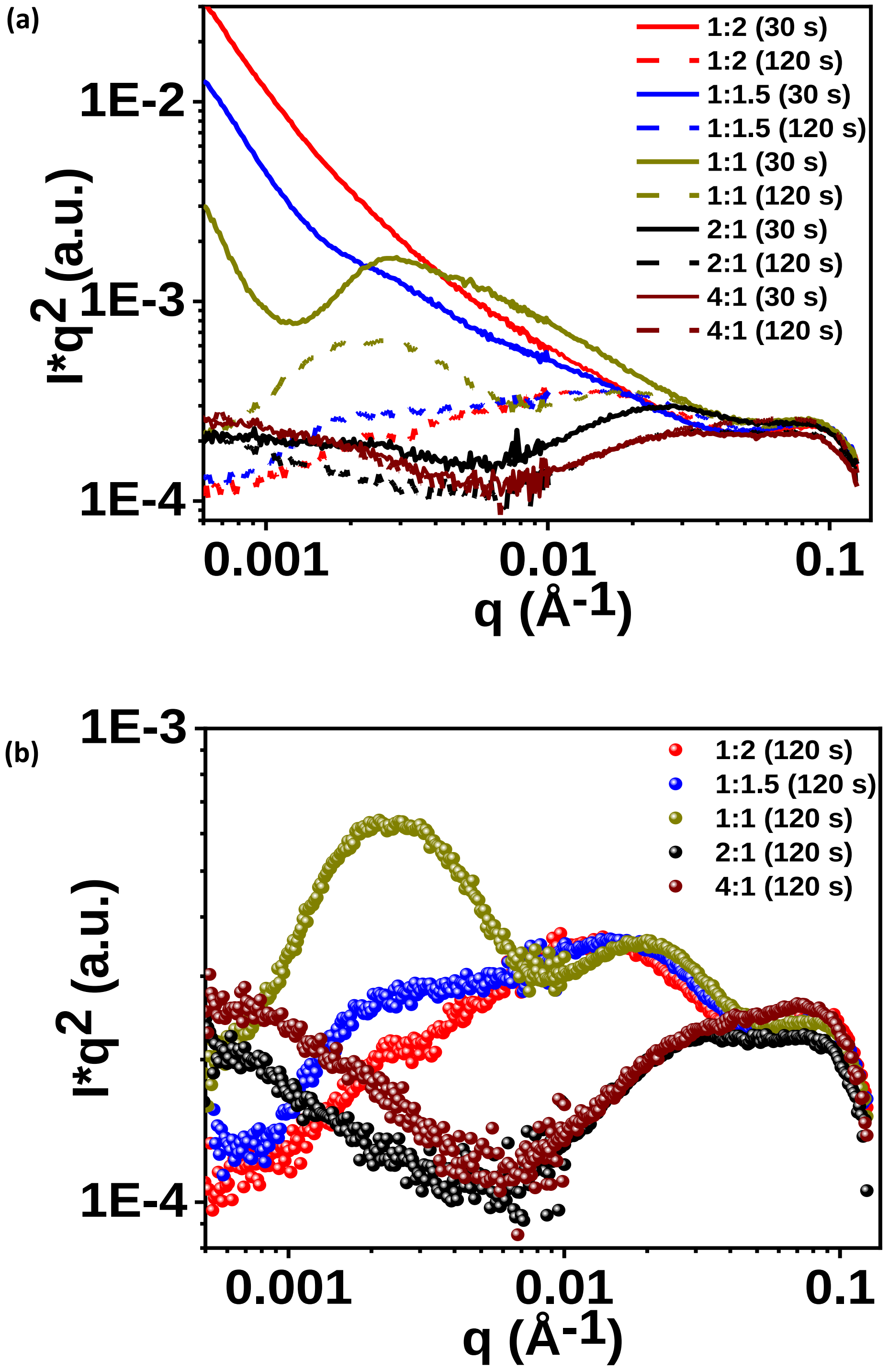

Figure S12. (a) Lorentz corrected R-SoXS profile of PTB7-Th:IEICO-4F films spin coated for 30 seconds and 120 seconds for different donor-acceptor ratio (1:2, 1:1.5, 1:1, 2:1, 4:1). **(b)** Lorentz corrected RSoXS profile for only fine films (120 s) for varied donor/acceptor blend ratio.

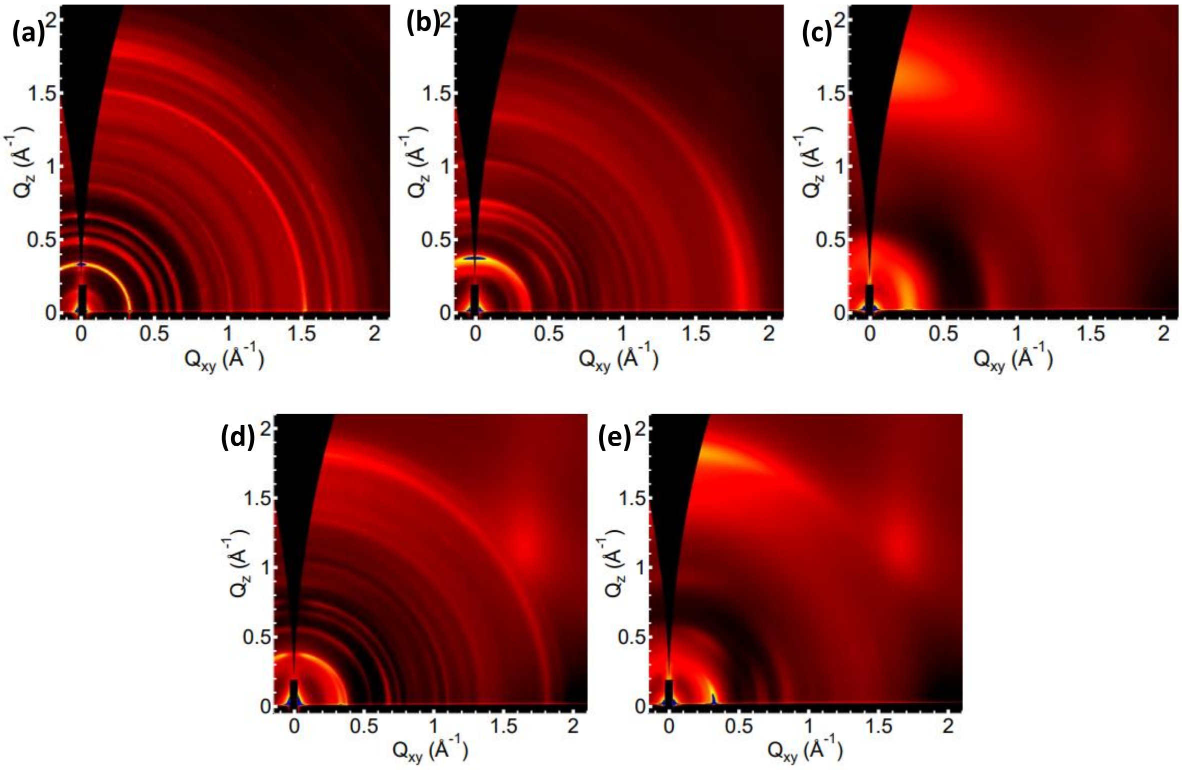

Figure S13. 2D GIWAXS profiles of **(a)** pristine IEICO-4F in CB, **(b)** pristine IEICO-4F in CB with 3% 1-CN, **(c)** pristine PTB7-Th in CB, **(d)** coarse blend film and **(e)** fine blend film processed from CB with 3% 1-CN film.

Table S1. Major GIWAXS peaks of fine and coarse blend morphology and their contribution from peaks of pristine materials.

	q (Å^{-1})	PTB7-Th	IEICO-4F	IEICO-4F with CN
Blend fine	0.27	✓	✗	✗
	0.32	✗	✓	✗
	1.58	✓	✗	✗
	1.82	✗	✗	✓
Blend coarse	0.27	✓	✗	✗
	0.33	✗	✗	✓
	0.38	✗	✗	✓
	1.82	✗	✗	✓

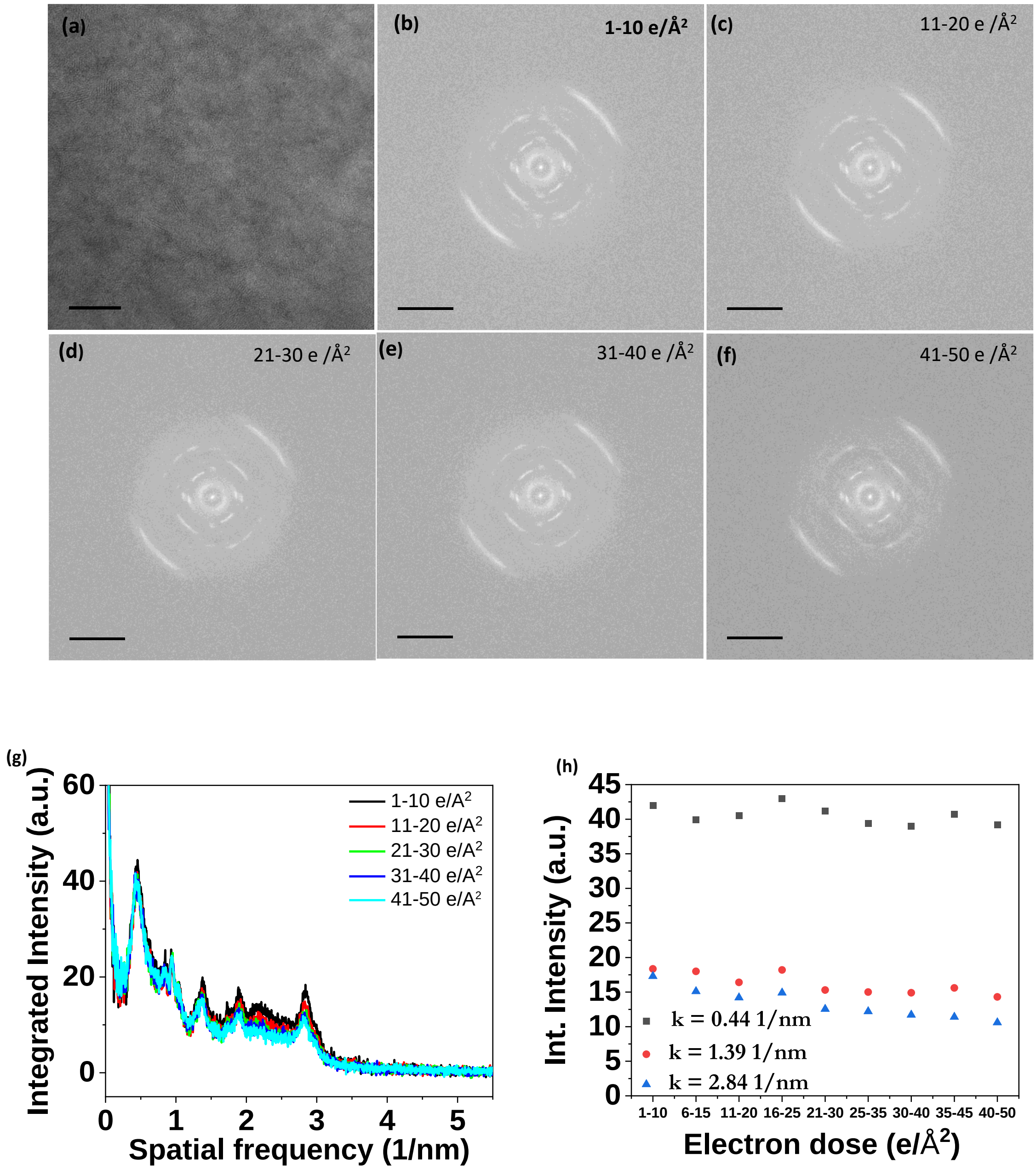

Figure S14. (a) High magnification cryo-EM image at the electron dosage of 50 e-/Å^2. FFT of the cryo-EM image at **(b)** 1-10 e/Å^{2,} **(c)** 11-20 e/Å^2, **(d)** 21-30 e/Å^2, **(e)** 31-40 e/Å^2 and **(f)** 41-50 e/Å^2, **(g)** Radial intensity profile of the FFT for the different rolling electron dosage. **(h)** Integrated intensity as a function of rolling electron dose for spatial frequency corresponding to 0.44, 1.39 and 2.83 1/nm.

Table S2. q value obtained from in-plane GIWAXS plot of coarse blend film and matched with q values obtained from the radial plot at different regions of the cryo-EM image. Green tick represents the q value which is present in the centre/edge/outside domain region of the blend film in cryo-EM image.

q (Å^{-1}) GIWAXS in-plane	**Cryo-EM centre**	**Cryo-EM edge**	**Cryo-EM outside**
0.265	✗	✓	✓
0.33	✓	✗	✓
0.381	✗	✓	✗
0.548	✓	✗	✗
0.678	✗	✓	✗
0.822	✓	✗	✓
0.885	✗	✓	✗
1.1	✓	✓	✗
1.34	✓	✓	✓
1.44	✓	✗	✓
1.8	✗	✓	✗

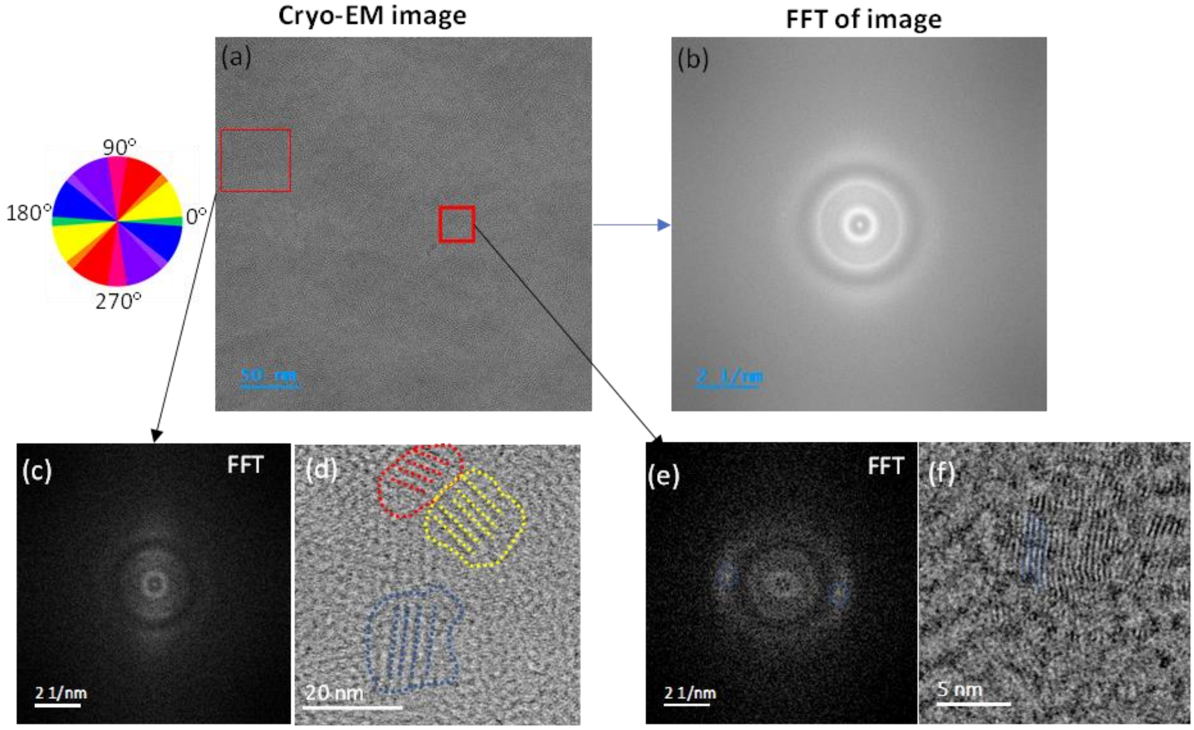

Figure S15. (a) Cryo-EM image and **(b)** its FFT from the matrix region of the coarse blend film. **(c)** FFT and its **(d)** inverse FFT from the small region showing crystalline fringes with low k spacings. The lamellar fringes are highlighted to show the different crystalline orientation. **(e)** FFT and **(f)** inverse FFT from another small region showing fringes from higher k-spacings. The colour-wheel corresponds to the angle of diffraction spots in the FFT of image.

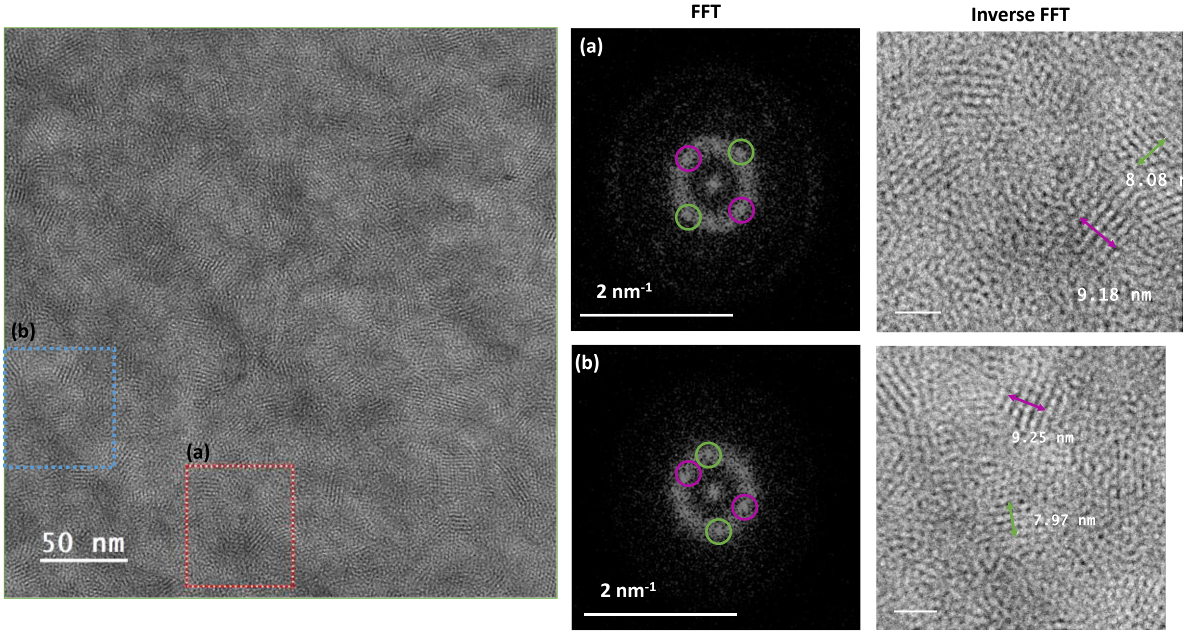

Figure S16. Cryo-TEM image acquired at the matrix region of the coarse blend film. FFT and inverse FFT of the sub-regions (a and b). The diffraction spot corresponding to IEICO-4F (100) and PTB7-Th (100) is highlighted in green and pink circle, respectively. Inverse FFT showing the fringe spacing of ~2 nm (IEICO-4F 100) and ~2.3 nm (PTB7-Th 100).

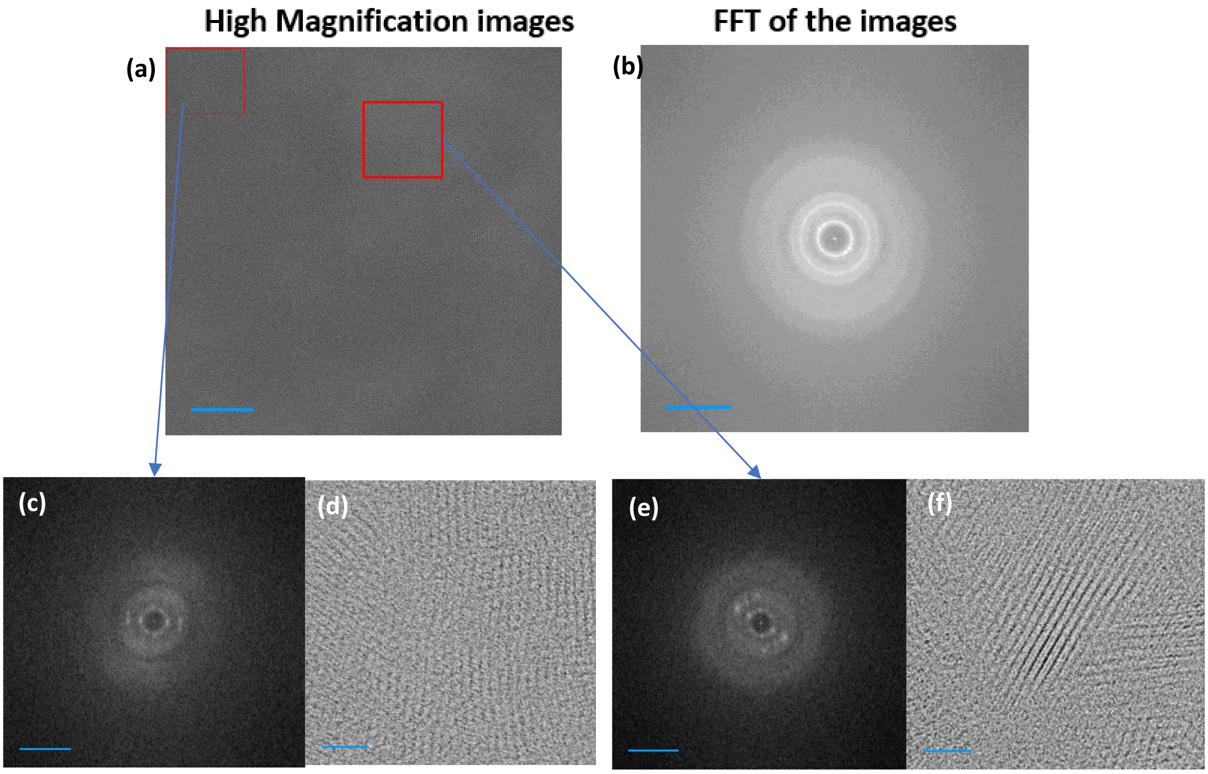

Figure S17. (a) Cryo-EM image and its **(b)** FFT from the fine blend morphology. **(c,e)** FFT and its **(d,f)** inverse FFT from the small regions of high magnification image showing crystalline fringes corresponding to different k-spacings.

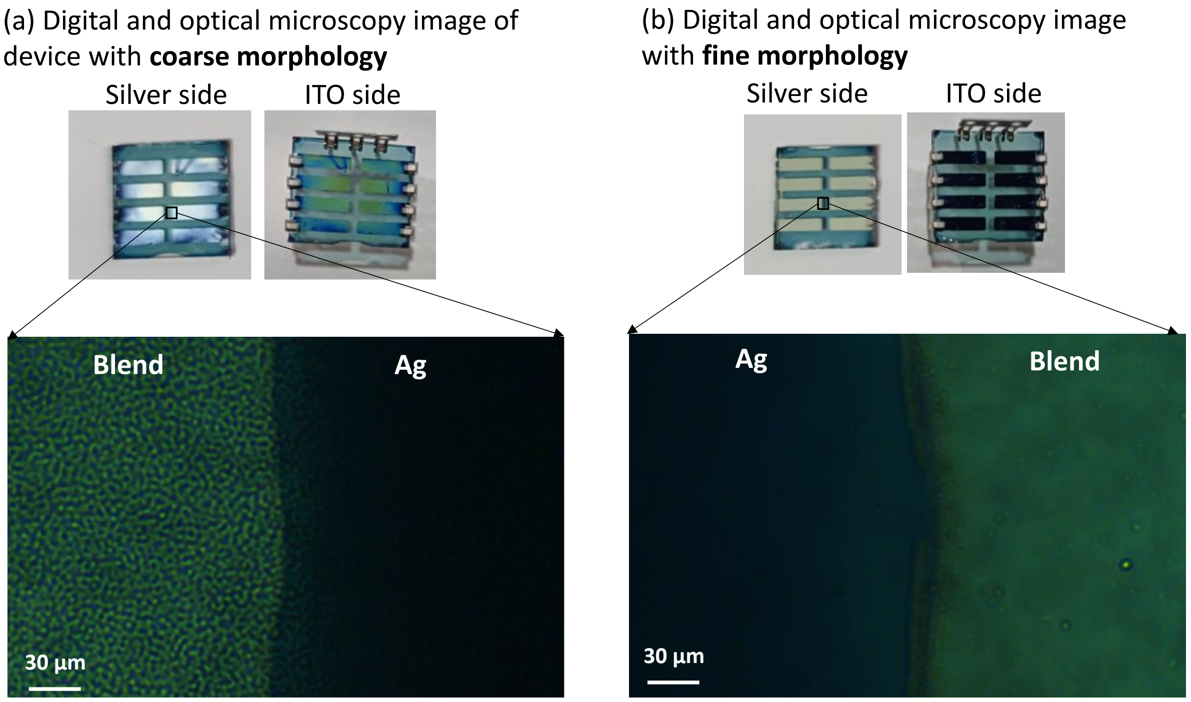

Figure S18. Digital image and optical microscopy image of device showing (a) matt-finish device with large phase-separated coarse blend morphology and (b) shiny-finish devices with fine blend morphology.

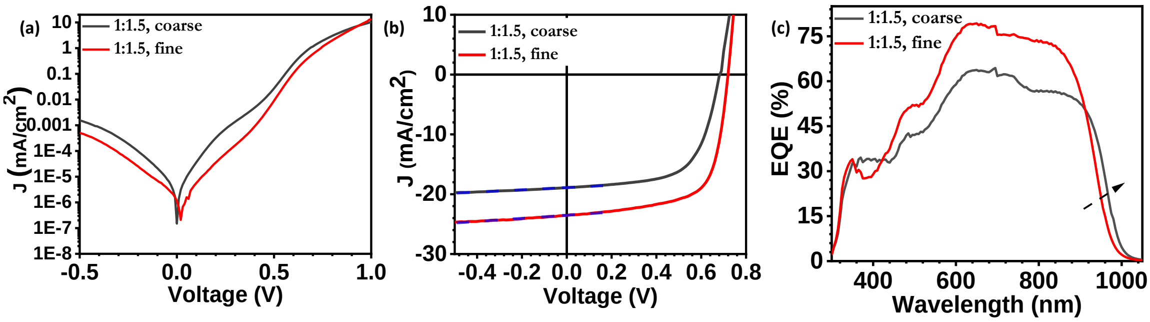

Figure S19. **(a)** Semi-log plot of dark J-V, **(b)** illuminated J-V, and **(c)** EQE of PTB7-Th:IEICO-4F 1:1.5 blend devices spin coated at 2000 rpm for 30 seconds (coarse) and 2000 rpm for 120 seconds (fine). Shunt resistance of devices is calculated by linear fitting of *J-V* curve at V=0. The shunt resistance is 420 Ω cm^2 for fine blend morphology and 520 Ω cm^2 for coarse blend morphology.

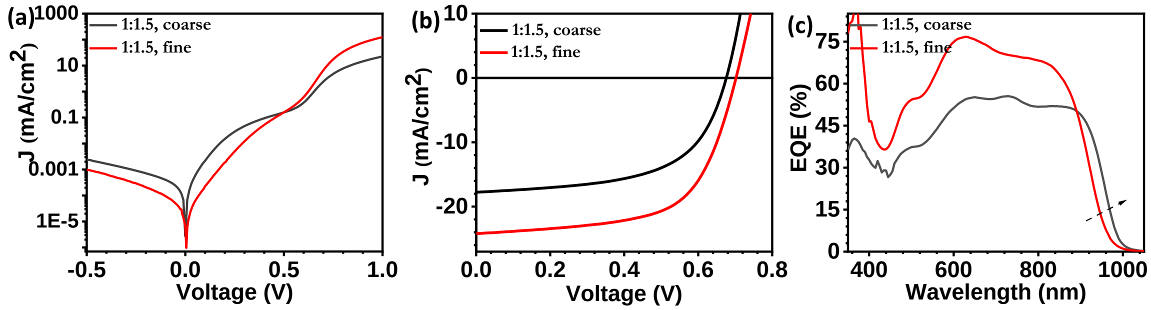

Figure S20. **(a)** Semi-log plot of dark *J-V*, **(b)** illuminated *J-V* and **(c)** EQE of PTB7-Th:IEICO-4F 1:1.5 blend devices spin coated at 1500 rpm for 30 seconds (coarse) and 1500 rpm for 120 seconds (fine).

Table S3. Extracted device performance parameters from *J-V* and EQE measurements for coarse and fine films of PTB7-Th:IEICO-4F devices spin-coated at 1500 rpm for 30 seconds and 120 seconds.

	J_{SC} (mA/cm^2)	V_{OC} (V)	FF (%)	PCE (%)	J_{SC} from EQE (mA/cm^2)
1500 rpm, 30 sec (coarse)	**17.7**	**0.68**	**58**	**7**	**17**
1500 rpm, 120 sec (fine)	**24**	**0.71**	**62.5**	**10.7**	**22.6**

Supplementary Note 3

Figure S21(a) shows log-log plot of J_{SC} and light intensity which are correlated by the expression $J_{SC} \propto I^{\alpha}$, where $\alpha<1$ implies J_{SC} is dependent on bimolecular recombination.[1] Figure S21(a) shows that the extracted α is 0.99 for both the devices implying insignificant bimolecular recombination in both the devices at short circuit condition. Therefore, the photocurrent losses in device are attributed to the monomolecular recombination (geminate recombination or trap-assisted recombination), mostly dominated by geminate recombination due to the high dielectric constant of organic materials.[2] The geminate recombination can be due to excitons recombining before they reach the interface or by geminate pairs at the D/A interface. The geminate recombination of the excitons before they reach interface is higher in the coarse morphology due to large domains resulting in higher PL counts (Figure S4(c)). However, the geminate recombination of the dissociated excitons at the D/A interface is strongly field dependent and is similar for both the blend films due to similar shunt resistance of devices (Figure S19(b)).[3]

Figure S21(b) shows the intensity dependent V_{OC} plot to gain insight on the non-geminate recombination in the devices. The slope of V_{OC} vs ln(I) is 1.42 k_BT/q for devices with fine morphology and 1.7 k_BT/q for devices with coarse morphology film. The slope of 1 k_BT/q signifies trap-free recombination and higher slope value implies trap-assisted charge recombination at open circuit voltage.

References:

1. Cowan, S. R.; Roy, A.; Heeger, A. J., *Physical Review B* **2010,** *82* (24).

2. R. A. Marsh, C. R. M., A. Abrusci, A. R. Campbell, and R. H. Friend, *Nano Letters* **2008,** *8*, 1393-1398.

3. Massip, S.; Oberhumer, P. M.; Tu, G.; Albert-Seifried, S.; Huck, W. T. S.; Friend, R. H.; Greenham, N. C., *The Journal of Physical Chemistry C* **2011,** *115* (50), 25046-25055.

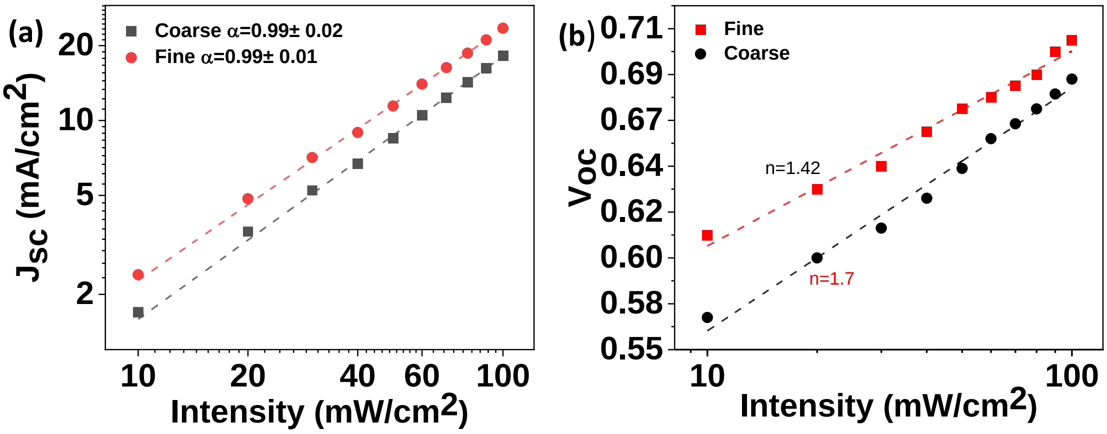

Figure S21. Light intensity dependent (a) short circuit current density and (b) open circuit voltage for PTB7-Th:IEICO-4F devices with coarse and fine morphology. The α is derived from expression $J_{SC} \propto I^{\alpha}$ by plotting J_{SC} and intensity in log-log plot and fitting with power law. The slope of V_{OC} with ln(I) gives slope of nkT/q from where n is derived.

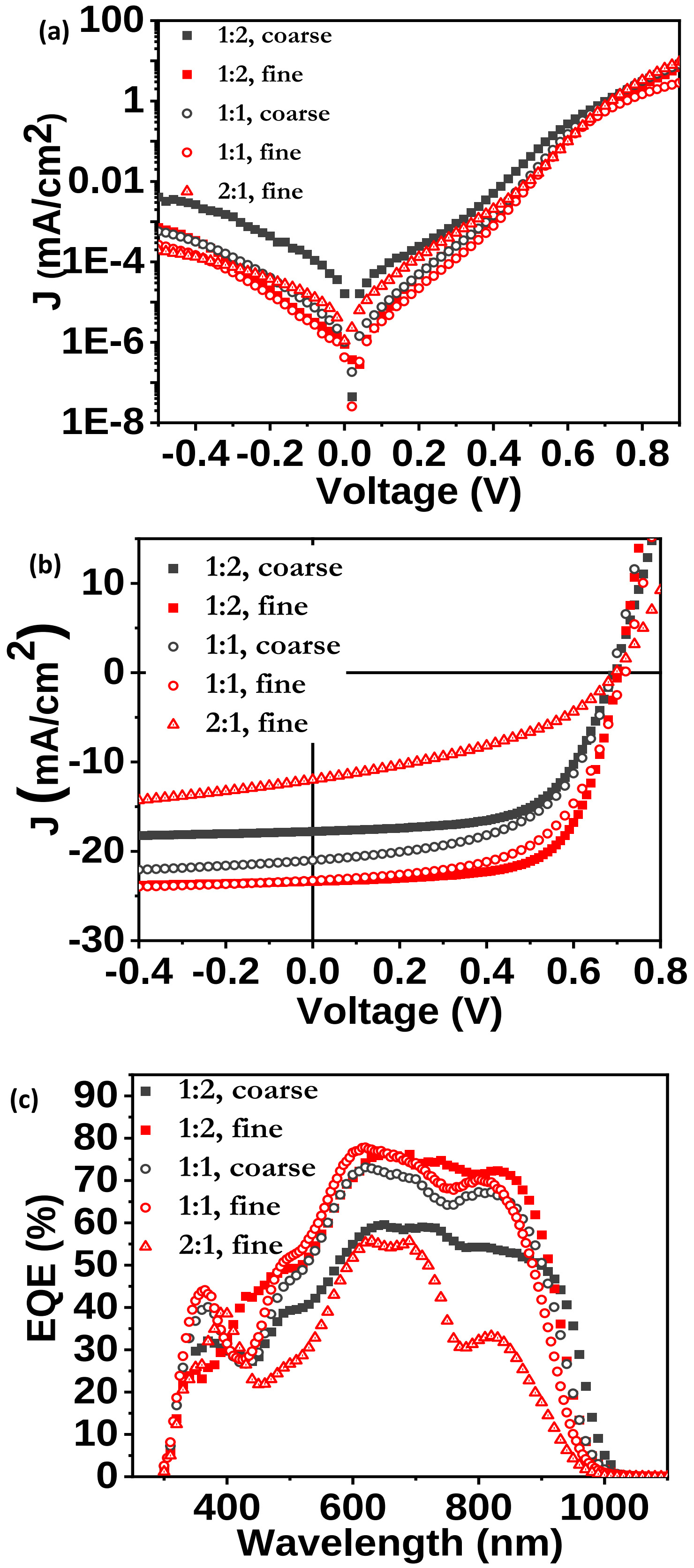

Figure S22. (a) Dark, **(b)** illuminated *J-V* characteristics and **(c)** EQE of PTB7-Th:IEICO-4F blend for 1:2, 1:1, and 2:1 blend ratio of coarse and fine films.

Table S4. Extracted performance parameters from *J*-*V* and EQE measurements coarse and fine films of PTB7-Th:IEICO-4F devices for 1:2, 1:1, and 2:1 blend ratio. Uncertainty is due to standard deviation of 10 samples.

	J_{SC} (mA/cm^2)	V_{OC} (V)	FF (%)	PCE (%)	J_{SC} from EQE (mA/cm^2)
1:2 (coarse)	17.7±2.6	0.68±0.01	58.2±3.3	7.0±1.2 (8.2)	17.3±2.4
1:2 (fine)	23.4±0.7	0.705±0.01	65.1±0.8	10.7±0.3 (11)	22.5
1:1 (coarse)	20.9±0.6	0.69±0.005	58.2±0.3	8.4±0.3 (8.7)	20.9
1:1 (fine)	23±0.5	0.71±0.005	55.9±1.9	9.1±0.6 (9.7)	21.8
2:1 (fine)	12.4±0.6	0.705±0.005	41.9±1.3	3.7±0.1 (3.8)	13

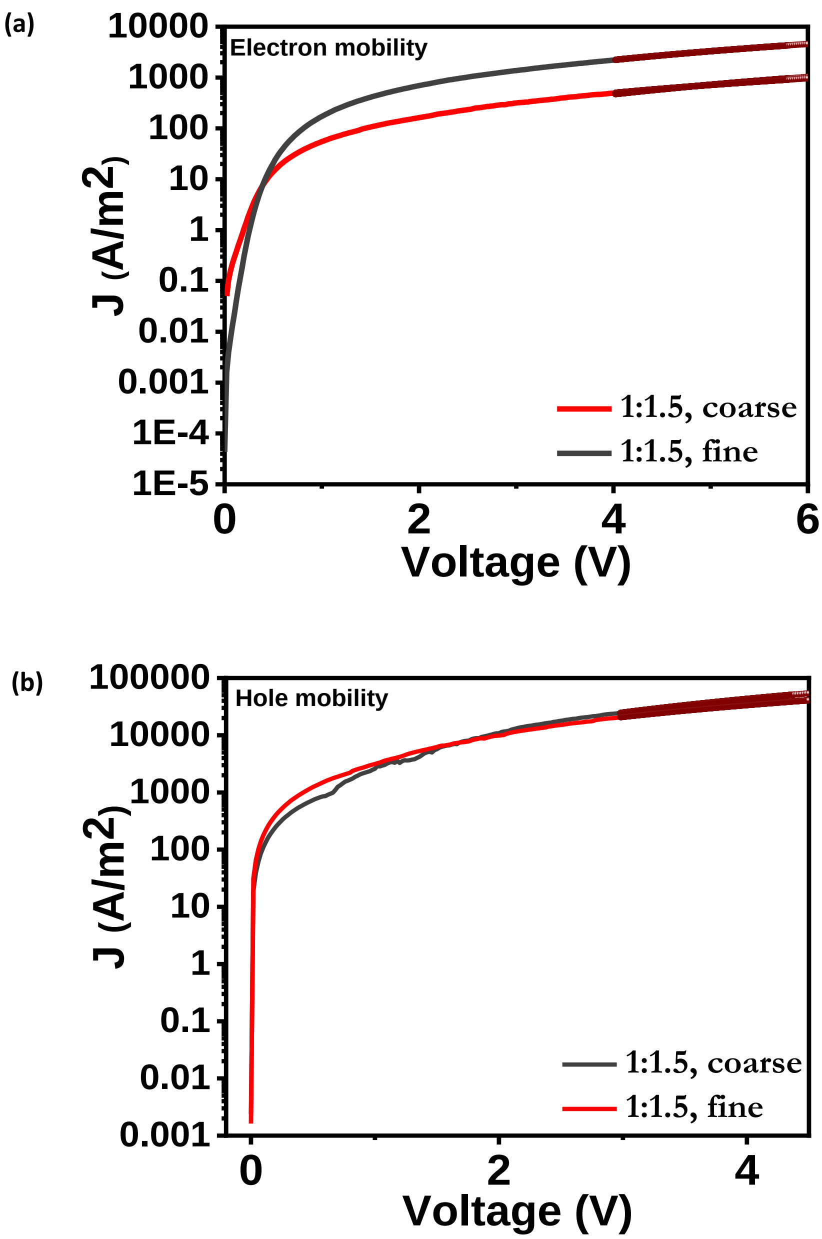

Figure S23. (a) *J-V* curve for electron only devices and **(b)** J-V curve for hole only devices of PTB7-Th:IEICO-4F (1:1.5) blend spin coated at 2000 rpm for 30 seconds (coarse) and 120 seconds (fine).

Supplementary note 4:

The electron- and hole-mobility are measured by fitting the single carrier *J*-*V* curves with the *Murgatroyd* equation, $J = \frac{\frac{9}{8}\boldsymbol{\varepsilon}\mu(\boldsymbol{V}-\boldsymbol{V}_{\boldsymbol{bi}})^2\boldsymbol{exp}(\boldsymbol{g}\sqrt{\boldsymbol{V}-\boldsymbol{V}_{\boldsymbol{bi}}})}{d^3}$, in which V_{bi} is the built-in potential, $\boldsymbol{\varepsilon}$ is the permittivity, $g = \frac{\beta}{\sqrt{d}}$ where β is the Poole–Frenkel coefficient, and *d* is the film thickness. The film thickness measured by the Dektak profilometer in coarse and fine blend morphologies at a 1:1.5 ratio is 90 nm. Table S4 shows the device performance of the 1:2 blend ratio, which is similar to the performance of the 1:1.5 blend ratio. In 1:1 blend system, the difference between the device performance of coarse and fine film is only 1 %, which is due to the reduced difference in the blend morphology. The electron mobility of blend films decreases from 2.2 X 10^{-5} cm^2/Vs to 0.36 X 10^{-5} cm^2/Vs when the blend ratio changes from 1:2 to 2:1. Interestingly, the electron mobility of pristine IEICO-4F films is lower than the mobility of blend films, which was also observed before by Wang et al. with a different polymer[1]. The improved electron mobility of IEICO-4F with PTB7-Th could be due to better electron transport in the blend, which provides a path for electron transport.

Reference:

1. Z. Wang, H. Jiang, X. Liu, J. Liang, L. Zhang, L. Qing, Q. Wang, W. Zhang, Y. Cao, J. Chen, *Journal of Materials Chemistry A* **2020**, 8, 7765.

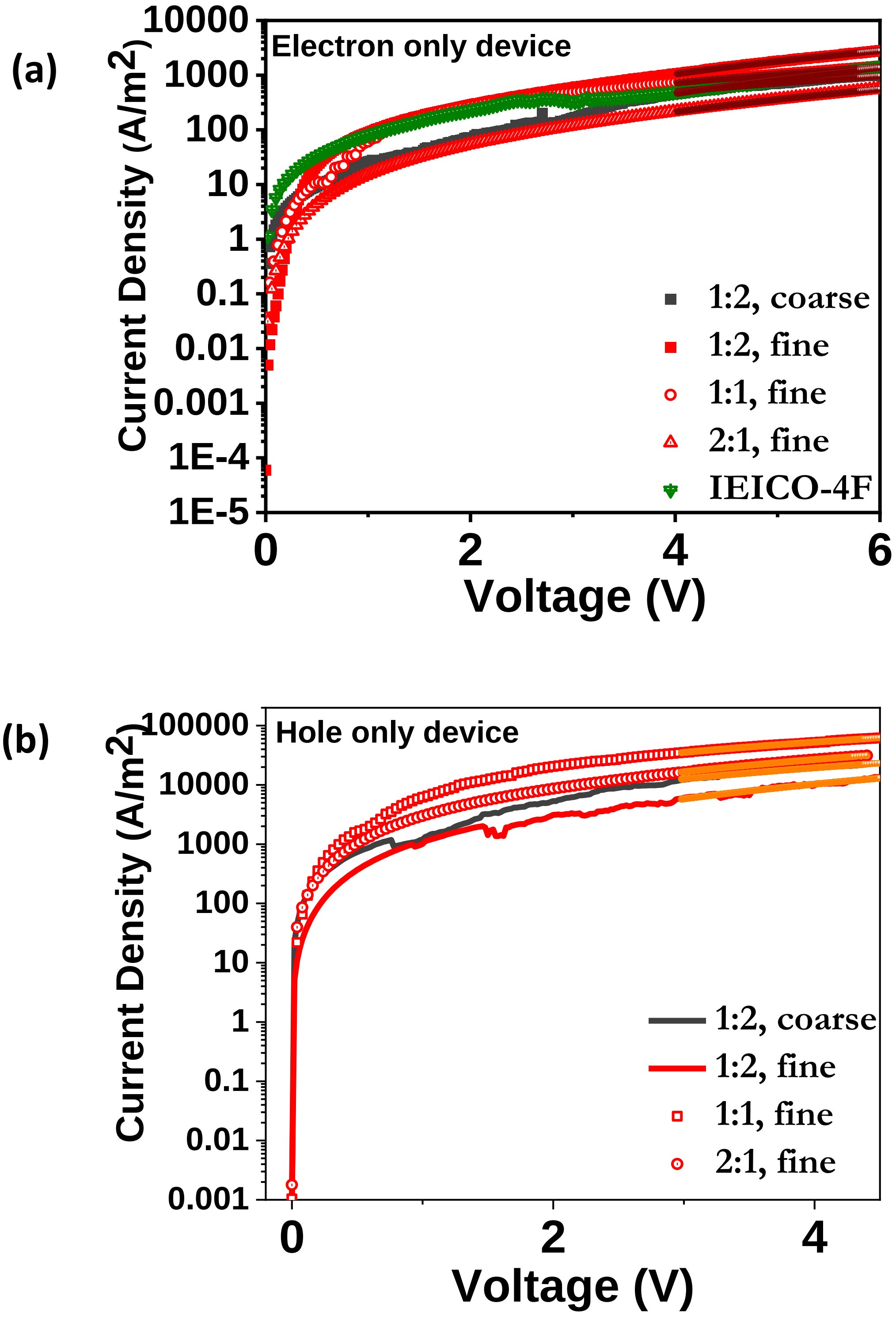

Figure S24. (a) *J-V* curve of electron-only devices , **(b)** hole-only devices for PTB7-Th:IEICO-4F blend in 1:2, 1:1 and 2:1 blend ratio of coarse and fine films along with pristine IEICO-4F. The line fits are obtained using *Murgatroyd* equation.

Table S5. Electron and hole mobility extracted from single carrier devices of pristine IEICO-4F and PTB7-Th:IEICO-4F blend in 1:2, 1:1, and 2:1 ratio. Uncertainty is due to standard deviation of 10 samples.

Device	**Electron mobility (cm^2/Vs)**	**Hole mobility (cm^2/Vs)**
1:2 1500 rpm, 30 sec	**(0.61±0.32) x 10^{-5}**	**(1.6±0.8) x 10^{-3}**
1:2 1500 rpm, 90 sec	**(2.2±0.9) x 10^{-5}**	**(7±2.6) x 10^{-4}**
1:1 1500 rpm, 90 sec	**(1.32±0.1) x 10^{-5}**	**(3.6±1.3) x 10^{-3}**
2:1 1500rpm, 90 sec	**(0.36±0.06) x 10^{-5}**	**(2.0±0.7) x 10^{-3}**
IEICO-4F	**(1.2±0.3) x 10^{-5}**	**-**

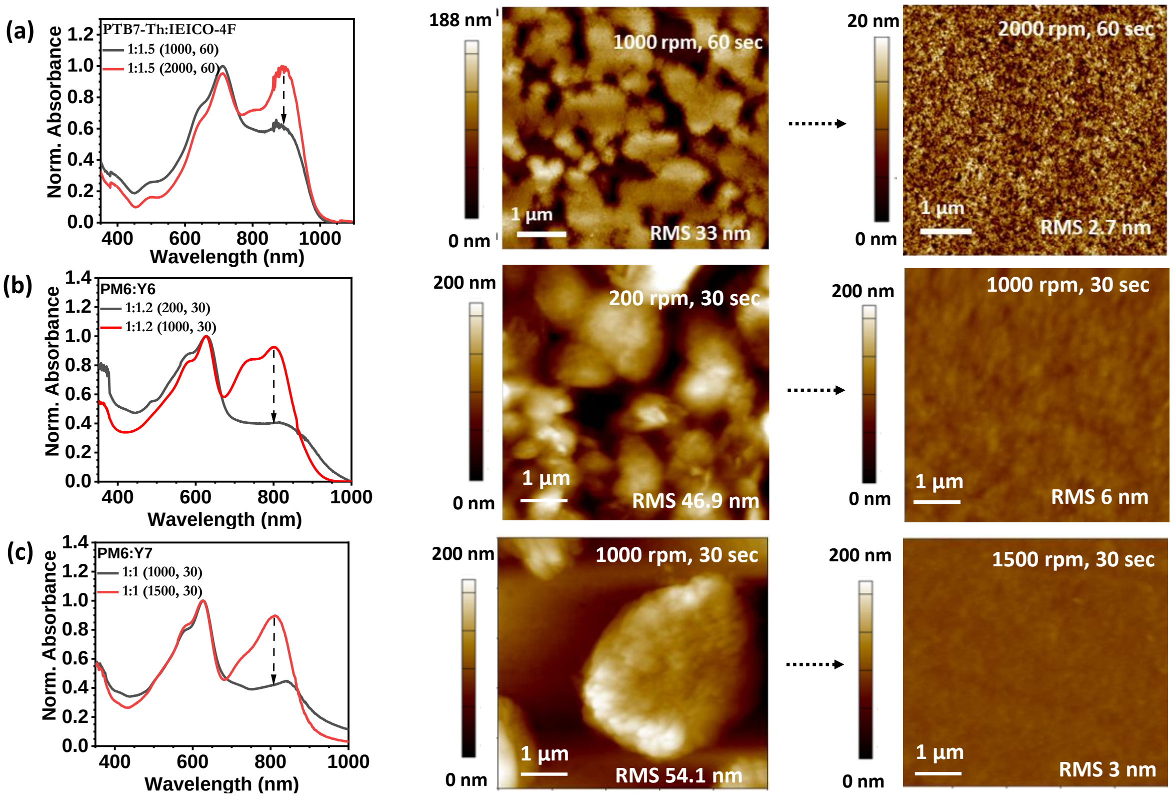

Figure S25. Absorption spectra and AFM height image for (a) PTB7-Th:IEICO-4F (1:1.5) in CB with 1-CN, (b) PM6:Y6 (1:1.2) in CF with 1-CN and (c) PM6:Y7 (1:1) in CB with 1-CN films spin-coated at different speed.

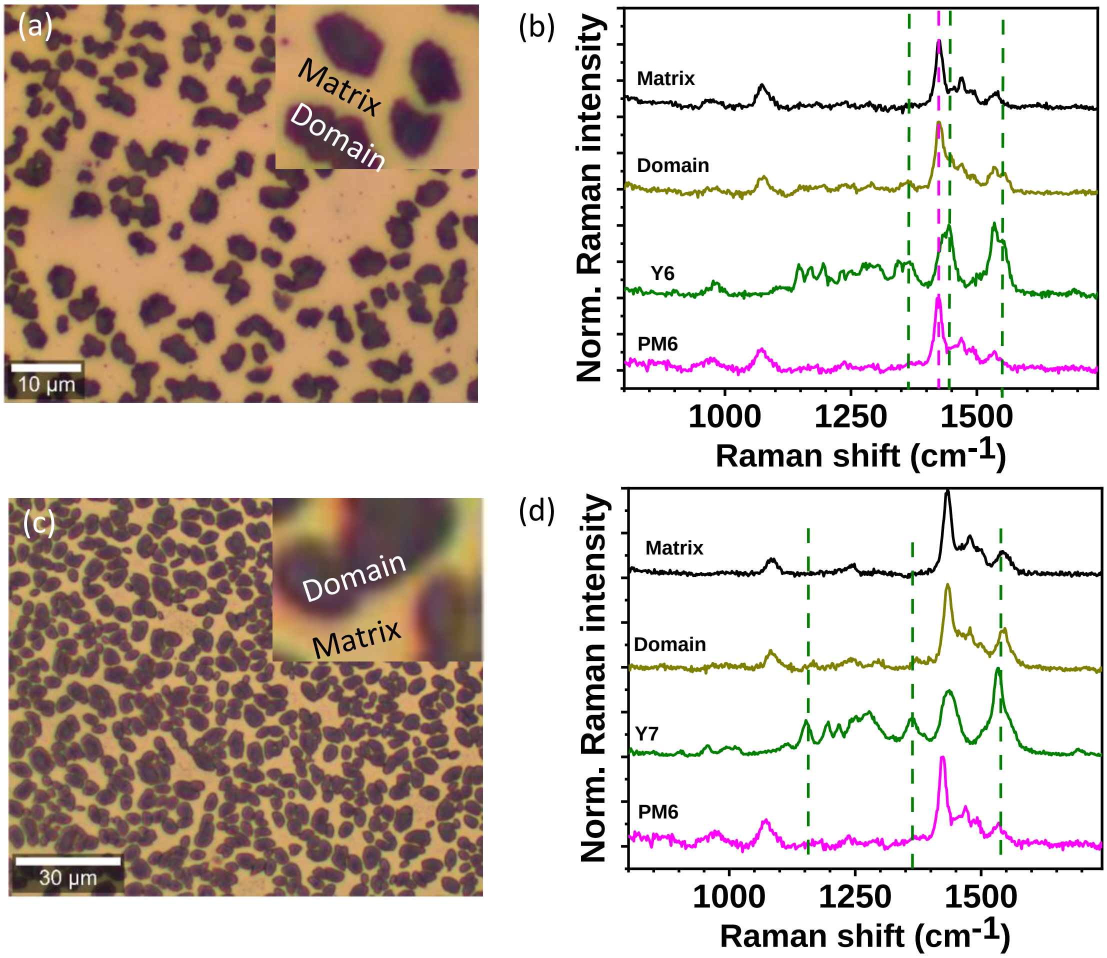

Figure S26. **(a)** Optical image of phase separated PM6:Y6 blend and **(b)** Raman spectra of pristine PM6, Y6, inside, and outside blend region. **(c)** Optical image of phase separated PM6:Y7 blend and **(d)** Raman spectra of pristine PM6, Y7, inside, and outside blend region.